



INTERACTION OF AEROELASTIC FORCES AND TURBULENCE AT FLUTTER ONSET WIND SPEED

M. Hunyadi* and I. Hegedűs

Department of Structural Engineering, Budapest University of Technology and Economics,
Műegyetem rkp. 3, H-1111 Budapest, Hungary

Received: 20 January 2012; **Accepted:** 5 May 2012

ABSTRACT

The investigation of the self-feeding forces impact on the structural displacements in turbulent wind is presented. This impact is dealt with as a ratio of the displacement variances with and without the self-feeding forces, and a formula is proposed for this ratio on a 2DOF section-model. The paper also presents a method to determine the softness of the flutter that affects significantly the impact of the self-feeding forces over the buffeting forces. This method highlights the influence of the flutter derivatives on how the structural parameters affect the softness.

Keywords: Flutter; turbulence; flutter wind speed; soft-type flutter; flutter softness

1. INTRODUCTION

Aeroelasticity deals with wind induced motions of structures when the motions considerably influence the aerodynamic forces acting at the structure. Characteristic occurrence of such motions is the flutter of aeroplane wings and bridge decks. Aeroelastic flutter is a complex self-feeding oscillation which may increase until the rupture of the oscillating structure. Flutter instability was first investigated for airplane wings in the thirties of the 20th century by Theodorsen [11]. He gave an analytic description of the phenomenon for flat plates in laminar flow.

After the collapse of a suspension bridge due to flutter instability (1940), Theodorsen's model aroused an expanding interest in the field of structural engineering too. On the basis of his results, Klöppel and Thiele [11] worked out a flutter analysis of bridge decks of various built-up. The description of the self-feeding forces has obtained a widely used format

* E-mail address of the corresponding author: hunyadi@vbt.bme.hu (M. Hunyadi)

developed by Scanlan et al. [22]. Their frequency domain analysis uses the so called aeroelastic flutter derivatives that have to be determined in wind tunnel tests. Scanlan's derivatives are useful tools for determining maximum values of admissible laminar wind velocity, however, their usability in turbulent wind problems needs a fairly complex improvement.

Until quite recently, most of the engineering methods for checking the flutter instability of bridges were based on the results of analyses obtained by two or three DOF (degree of freedom) bridge deck models exposed to the impact of laminar flow. Effects of the real wind structure on the flutter velocity can be taken into consideration by factors that take into account the coherence, the limited persistence of blast forces, etc., even so, the estimated velocities had to keep a considerable safety margin and are inadequate for service state analysis.

Theoretical background for time domain description of the phenomenon (through Sears and Wagner functions) was parallelly developed [3]. Contrasting terms "time domain" and "frequency domain" refer to a basic difference in approaches: time domain description focuses on changes over time, whereas a frequency domain description tells us how can be the changes decomposed into periodic constituents of different frequencies and phases. Both descriptions can be considered as complete, however, in concrete problems one or the other can prove more efficient.

Computer aided flutter analyses have evolved in increasing level of adequacy: steady theory, quasi steady theory, the description of the flutter derivatives by convolution integrals, etc. [4]. Time domain description of the self-feeding forces permits their treating combined with the effects of the turbulent wind field. As convolution integrals are time and storage consuming methods also alternative algorithms were developed. Chen and Kareem [5,6] have presented a method based on a frequency independent rational function approximation of the self-feeding forces, thus no convolution is required in the calculation.

Numerical simulation of turbulent wind fields superimposes trigonometric functions of amplitudes determined by the power density function (PSD) of the wind. Advanced algorithms use white noise convolution based simulation for complex structures [7], some time domain simulations use various decompositions of the PSD (eg. proper orthogonal decomposition, POD [1, 8, 9]), others use the ARMA representation of wind [10,11].

The structural response due to turbulent flow has to be analyzed in service states too. When the design wind speed and the flutter velocity get close the influence of the flutter on the structural response may become important. Although this influence has been examined in some papers (e.g. in [4,5]), handy estimating methods widely used in other fields of structural stability analysis have not yet been worked out.

This paper presents a proposed model to estimate the structural responses due to self-feeding forces in turbulent flow.

2. THEORETICAL BACKGROUND

The structural responses to wind forces depend on the spatial and temporal properties of the structure and the wind field. Nevertheless, a section-model is in general sufficient to the analysis of the aerodynamic instability of a bridge deck. Furthermore, scientific papers have

demonstrated that the vertical displacement and torsional rotation around the span-wise axis is enough to describe the effects of the self-feeding forces. The lateral along-wind displacement is an extension to the model as a third degree of freedom, and is needed to be taken into account only for very long bridges.

In the following a 2DOF section-model is dealt with for buffeting and self-feeding forces, with the two degrees as h for the vertical displacement and α as the torsional rotation around the centre of gravity of the symmetric cross section, see Figure 1. The average wind is supposed to be horizontal ($\alpha=0$ incidence) and to be perpendicular to the span-wise axis.

2.1 Spectral turbulence analysis

The self-feeding forces depend on the displacement of the structure, a feedback is present in the forces. Thus only the buffeting forces are investigated in the spectral analysis. By considering the wind field as an ergodic stationary process, the power spectral density (PSD) of the wind speed fluctuation is considered as the input to the spectral system. Supposing the structural behaviour as being linear the PSD of the displacement vector \mathbf{x} is expressed in the form

$$\mathbf{S}_x(\omega) = \mathbf{H}^*(\omega) \mathbf{S}_{f_b}(\omega) \mathbf{H}^T(\omega) \tag{1}$$

where \mathbf{S}_{f_b} is the PSD of the buffeting forces, $\mathbf{H}(\omega)$ is the transfer function matrix, ω is the circular frequency, $()^*$ and $()^T$ represent the complex conjugate and transpose, resp. The variance of the displacements is

$$\sigma_x^2 = \frac{1}{2\pi} \int_0^\infty \mathbf{S}_x(\omega) d\omega \tag{2}$$

2.2 Buffeting forces in the time domain analysis

The buffeting forces acting on the section-model have the form [12]

$$\mathbf{f}_b(t) = \frac{1}{2} \rho U^2 \mathbf{B} \mathbf{C}_b \frac{\mathbf{u}(t)}{U} \tag{3}$$

$$\mathbf{B} = \begin{bmatrix} B & 0 \\ 0 & B^2 \end{bmatrix} \quad \mathbf{C}_b = \begin{bmatrix} -2C_L & -(C_L' + C_D) \\ 2C_M & C_M' \end{bmatrix} \tag{4}$$

where \mathbf{C}_b is the force coefficients matrix, C_D , C_L and C_M are the drag, lift force and torsional moment coefficients of the cross section, resp., at the angle of incidence $\alpha=0$ for the static equilibrium position and referred to the width B of the cross section, $()'$ represents the derivation according to the rotation α , $\rho=1.25$ kg/m is the air density at 20°C, $\mathbf{u}(t)=[u(t) \ w(t)]^T$ is the fluctuating wind speed vector. The aerodynamic admittance function takes into account the change in wind pressure caused by eddies of different frequencies. To have comparable results between the spectral analysis and the time domain analysis the admittance function has been omitted. The sign of the lift force in eq. (4) has been changed compared to the usual formulation of the buffeting forces due to the transformation to the coordinate system used for flutter description, as shown in Figure 1.

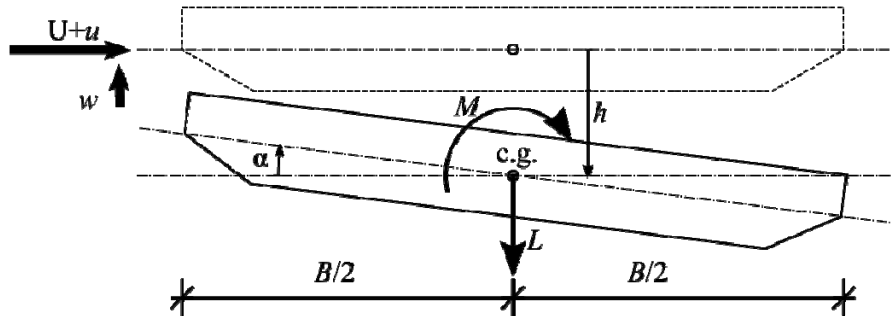


Figure 1. Definition of coordinates and displacements of the cross section

2.3 Self-feeding forces

The self-feeding lift force and pitching moment are expressed by the frequency dependent aeroelastic flutter derivatives as a linear function of the structural motion [2] in the matrix form

$$\mathbf{f}_{ae}(t) = \frac{1}{2} \rho U^2 \mathbf{B} (\mathbf{A}_s \mathbf{R} \mathbf{x}(t) + \mathbf{A}_d \mathbf{R} \dot{\mathbf{x}}(t)) \quad (5)$$

$$\mathbf{A}_s = K^2 \begin{bmatrix} H_4^* & H_3^* \\ A_4^* & A_3^* \end{bmatrix} \quad \mathbf{A}_d = K \begin{bmatrix} H_1^* & H_2^* \\ A_1^* & A_2^* \end{bmatrix} \quad \mathbf{R} = \begin{bmatrix} 1/B & 0 \\ 0 & 1 \end{bmatrix} \quad (6)$$

where the matrix \mathbf{R} transforms the displacement vector $\mathbf{x}(t) = [h(t) \ \alpha(t)]^T$ dimensionless, the dot represents the derivation according to time t , \mathbf{A}_s and \mathbf{A}_d are the aeroelastic stiffness and damping matrix, resp., defined by the heave and torsional flutter derivatives H_i^* and A_i^* ($i=1, \dots, 4$), resp. $K = \omega B/U$ is the reduced frequency where ω is the frequency of the (damped) harmonic oscillation of the cross section.

2.4 Approximation of the flutter derivatives

The assumption of a purely harmonic motion of the cross section involves that the previously introduced aeroelastic damping matrix gets multiplied by the (reduced) frequency and the imaginary unit. Thus the two aeroelastic matrices can be merged into one complex valued aeroelastic matrix, which, following the works of Chen et al. [5], is then approximated by frequency independent formulation. Therefore the flutter derivatives are approximated by rational functions as

$$K^2 \begin{bmatrix} H_4^* + iH_1^* & H_3^* + iH_2^* \\ A_4^* + iA_1^* & A_3^* + iA_2^* \end{bmatrix} = \mathbf{A}_1 + \mathbf{A}_2(iK) + \mathbf{A}_3(iK)^2 + \sum_{l=1}^m \frac{\mathbf{A}_{l+3} iK}{iK + d_l} \quad (7)$$

where $i = (-1)^{1/2}$ is the imaginary unit, \mathbf{A}_1 , \mathbf{A}_2 and \mathbf{A}_3 are related to the additional aeroelastic stiffness, damping and mass respectively, \mathbf{A}_l ($l=1, \dots, m$) represent the unsteady characteristics of the self-feeding forces, d_l ($d_l \geq 0$) constants approximate the time delays of the lag of the self-feeding forces and the velocity components. Consequently the frequency

independent representation of the self-feeding forces conforms to the time domain analysis.

Although the rational function approximation of the self-feeding forces is valid for the assumption of oscillating motions with small positive or negative damping, the numerical examinations showed good accordance of the flutter speed with the complex eigenvalue analysis. Since the proposal of the referenced work [5] the authors have not found discussions in regard to this theoretical discordance.

2.4 Equation of motion

Employing the rational function approximation of the self-feeding forces, the governing equation of motion becomes

$$\mathbf{M}_1 \ddot{\mathbf{z}} + \mathbf{C}_1 \dot{\mathbf{z}} + \mathbf{K}_1 \mathbf{z} = \mathbf{f} \tag{8}$$

where the terms \mathbf{M}_1 , \mathbf{C}_1 and \mathbf{K}_1 comprise the aeroelastic additional matrices as follows, the states space vector \mathbf{z} includes the displacements extended by the unsteady self-feeding force coefficients, and \mathbf{f} is the buffeting force vector:

$$\mathbf{M}_1 = \begin{bmatrix} \overline{\mathbf{M}} & \mathbf{0} & \dots & \mathbf{0} \\ \mathbf{0} & \dots & \dots & \mathbf{0} \\ \vdots & \vdots & \ddots & \vdots \\ \mathbf{0} & \dots & \dots & \mathbf{0} \end{bmatrix} \quad \mathbf{C}_1 = \begin{bmatrix} \overline{\mathbf{C}} & \mathbf{0} & \dots & \mathbf{0} \\ -\mathbf{A}_4 \mathbf{R} & \mathbf{I} & \mathbf{0} & \vdots \\ \vdots & \mathbf{0} & \ddots & \mathbf{0} \\ -\mathbf{A}_{l+m} \mathbf{R} & \mathbf{0} & \dots & \mathbf{I} \end{bmatrix} \tag{9}$$

$$\mathbf{K}_1 = \begin{bmatrix} \overline{\mathbf{K}} & -p\mathbf{B} & -p\mathbf{B} & -p\mathbf{B} \\ \mathbf{0} & \frac{Ud_1}{B} \mathbf{I} & \mathbf{0} & \mathbf{0} \\ \vdots & \dots & \ddots & \mathbf{0} \\ \mathbf{0} & \dots & \mathbf{0} & \frac{Ud_m}{B} \mathbf{I} \end{bmatrix} \quad \mathbf{f} = \begin{bmatrix} \mathbf{f}_b \\ \mathbf{0} \\ \vdots \\ \mathbf{0} \end{bmatrix} \quad \mathbf{z} = \begin{bmatrix} \mathbf{x} \\ \mathbf{x}_{ae,1} \\ \vdots \\ \mathbf{x}_{ae,m} \end{bmatrix} \tag{10}$$

where \mathbf{M} , \mathbf{C} and \mathbf{K} are the mass, damping and stiffness matrix resp., \mathbf{x} is the displacement vector, \mathbf{f}_b is the buffeting force vector, $\mathbf{x}_{ae,l}$ are the state space extension vectors representing the unsteady properties of the self-feeding forces and $p=1/2\rho U^2$ is the wind pressure.

The overlined mass, damping and stiffness terms merge the structural and aeroelastic properties as given by the equations

$$\overline{\mathbf{M}} = \mathbf{M} - 1/2\rho B^2 \mathbf{B} \mathbf{A}_3 \mathbf{R} \tag{11}$$

$$\overline{\mathbf{C}} = \mathbf{C} - 1/2\rho U B \mathbf{B} \mathbf{A}_2 \mathbf{R} - \sum_{l=1}^m 1/2\rho U^2 \frac{B}{Ud_l} \mathbf{B} \mathbf{A}_{l+3} \mathbf{R} \tag{12}$$

$$\overline{\mathbf{K}} = \mathbf{K} - 1/2\rho U^2 \mathbf{B} \mathbf{A}_1 \mathbf{R} \tag{13}$$

The previously presented system of equations can be solved by the Newmark- β method. In the structural instability analysis of compressed columns a factor based on the

Southwell method is used to estimate the second order effects. Similarly, the factor taking into account the contribution of the self-feeding forces to the buffeting forces is investigated. The squared ratio of the displacement variances under turbulent winds with/without the aeroelastic forces is defined as

$$\Psi^2 = \sigma_{x,b+ae}^2 / \sigma_{x,b}^2 \quad (14)$$

where $\sigma_{x,b}^2$ is the displacement variance due to buffeting forces only, and the one with index $b+ae$ refers to variances due to the buffeting and the self-feeding forces. The variances need to be calculated with spectral analysis for the case of the buffeting forces only, and by averaging several runs with randomly generated wind speed histories using time domain analysis in the case of inclusion of the self-feeding forces.

3. CALCULATIONS

Numerical calculations have been done to determine the above defined ratio of the displacements with/without the self-feeding forces in turbulent winds. The displacements of 2DOF cross-sections were investigated.

The parametric investigation has been done with several different structural configurations as follows:

- mass ratio $\mu=4m/\rho B^2\pi$ takes the values $\mu=10, 30, 50, 100$, where m is the mass of the section per unit length.
- dimensionless radius of gyration $r_\alpha=2(I/m)^{1/2}/B$ can have values of $r_\alpha=0.5, 0.75, 1.0$, where I is the rotational inertia around the centre of gravity.
- ratio of eigenfrequencies $\varepsilon=\omega_{0\alpha} / \omega_{0h} = 1.5, 2.0, 2.5$, where $\omega_{0\alpha}$ and ω_{0h} are the eigenfrequencies of the structure of the mode shapes of rotation and heave motions respectively.
- values of $\omega_{0h} = 1.0, 1.5, 2.5$ rad/s for the eigenfrequency of the heave mode shape are taken into account.
- logarithmic decrement of the structural damping in both rotation and heave modes is supposed to have the values of $\delta_s = 0.1, 0.01, 0.001, 0.0001$.
- width of the section set to $B=5$ m or 20 m.

Not all, but only 120 combinations of the above values has been dealt with. The concept of the combinations was to have all combinations with the settings $\varepsilon=1.5$, $B=5$ m and $\delta=0.01$, as these values are in the mid-range for typical footbridges. Other combinations were done by changing only one parameter from these settings.

According to [13] the one-sided PSD of the wind field was

$$\frac{nS_v(n)}{\sigma_v^2} = \frac{\lambda_v f_{L,v}}{(1+1.5\lambda_v f_{L,v})^{5/3}} \quad (v = u, w) \quad (15)$$

where n is the frequency, u and w refer to the along-wind and vertical speed fluctuations respectively, $f_{L,v}=nL_v/U$ is the dimensionless frequency. The settings of $L_u=200$ m and

$L_w=20$ m for integral lengths, $\sigma_u/U=0.10$ and $\sigma_w/U=0.05$ for turbulence intensity, coefficients $\lambda_u=6.868$ and $\lambda_w=6.103$ were used. As the cross-spectral density has no significant influence on the structural response [5], it has been omitted. The steady force coefficients of the cross section were $C_D = 0.3230$, $C_D'=0$, $C_L=0.0942$, $C_L'=1.905$, $C_M=0.0104$ and $C_M'=0.2717$.

Wind speed histories were generated by a POD based convolution of white noise signals given in [8] with $N_t = 2^{14}$ time steps of $\Delta t=0.04$ s each, which result in the lowest frequency of 1.525×10^{-3} Hz and the upper cut-off frequency of 12.5 Hz, thus numerically representing almost 93% of the energy given in the PSD. $N_{\text{POD}}=50$ POD eigenvalues were used for the interpolation.

The self-feeding forces are calculated according to the derivatives of a thin airfoil [1,3] using the rational function approximation given in (7).

3.1 Flutter speed criterion

The time histories of the structural responses (the displacements) are split into intervals of different lengths. The flutter speed is defined as the wind speed when the structural response has constant variances over these time intervals. Below the flutter speed these variances are decreasing functions, above the flutter speed they are increasing functions of the time interval length. This definition holds for analyses with and without turbulence.

The flutter speeds in absence of turbulence matched the ones determined by the complex eigenvalue analysis. The displacements' variances for the buffeting forces only were also checked against the spectral analysis and good accordance has been met.

3.2 Structural response with and without self-feeding forces

Twenty calculations were done with randomly generated wind fields at every setting of the structural parameters and at a given average wind speed. The wind speeds are set relative (mostly at around 100% with steps of 1%) to the flutter speed determined on the undamped structure by the complex eigenvalue analysis. In all cases torsional branch flutter occurred, as is typical for airfoils, with different phase shifts between the heave and angular motions. The variances of the heave motion showed slightly different flutter speed values than for the angular motion. This can be due to the lag between the two motion modes. Although it is remarked that the shape of the diagrams look different for the two motions, as is resulted by other authors (e.g. [14]), the diagrams of the variance of the rotational motion is steeper compared to the heave motion approaching to the critical velocity, which fact can be assigned to the torsional branch property of the flutter (see Figure 2a).

The squared ratio of the variances calculated with the self-feeding forces by time domain analysis and without them by spectral analysis is defined in eq. (14). A typical diagram of the ratio is shown in Figure 2b. The results show that instead of having the buffeting forces change the flutter speed while the displacements of the former remains unaltered, the aeroelastic damping significantly modifies the displacements due to the buffeting forces well below the change flutter speed. Near the flutter speed the two type of forces interact and the displacements increase. As the flutter in all configurations was of torsional type, the ratio ψ for the torsional motion had always greater value than for the heave motion.

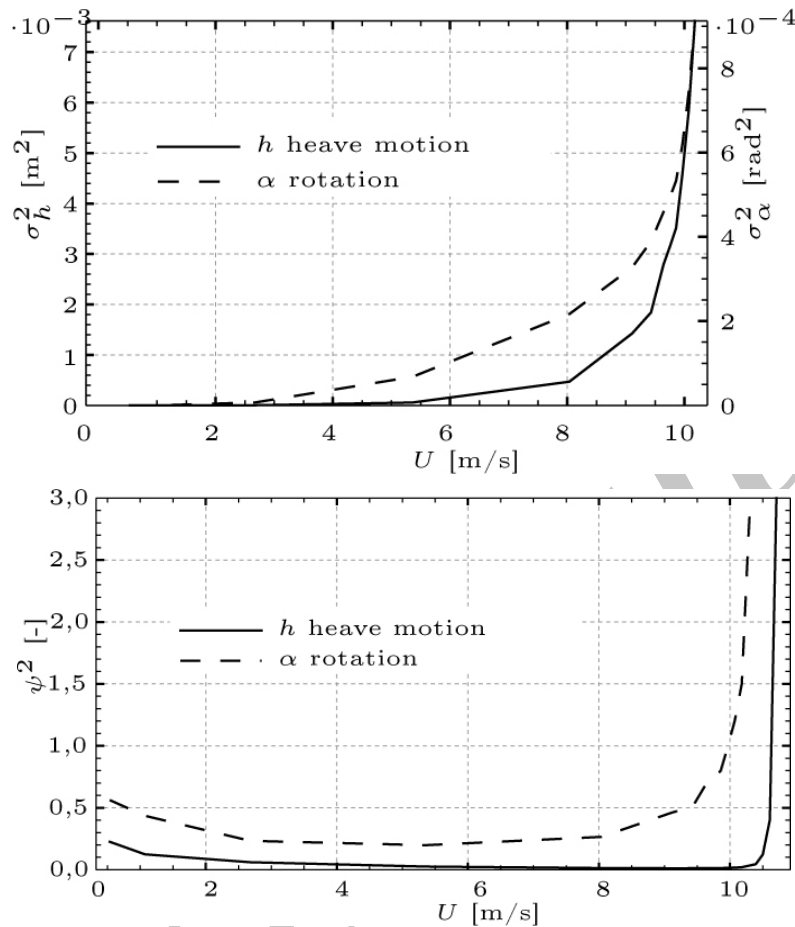


Figure 2. Heave and torsional motions in function of average wind speed until the flutter speed $U_F=10.20$ m/s is reached. Settings: $\mu=10$, $\varepsilon=1.5$, $r_\alpha=1.00$, $B=5$ m, $\omega_{0h}=1.5$ rad/s and $\delta_s=0.01$
 Top: Variances of the motions, below: Ratios of the variances with/without self-feeding forces

Such diagrams have been constructed for every structural configuration and are regarded as functions of the dimensionless relative speed as the ratio of the average wind speed and the estimated flutter speed. From the several structural settings it can be concluded that the dimensionless mass ratio delays the ratio of the motions, their diagram show lower values at the same relative speeds at greater mass ratios. The mass ratio has greater impact of the ratio of the angular motion than on the heave one. The same observation applies for the case of the width of the section, with much slower intensity. The dimensionless radius of gyration has an opposite effect: the ratio of the torsional motion increases much faster at lower relative velocities, but it seems to have no action in the case of the heave motion, which asserts the engineering intuition. The frequency ratio and the eigenfrequency (the heave motional, and through the frequency ratio the torsional eigenfrequency also) have no great effect on the diagrams, it appears to have an impact only on the flutter speed itself.

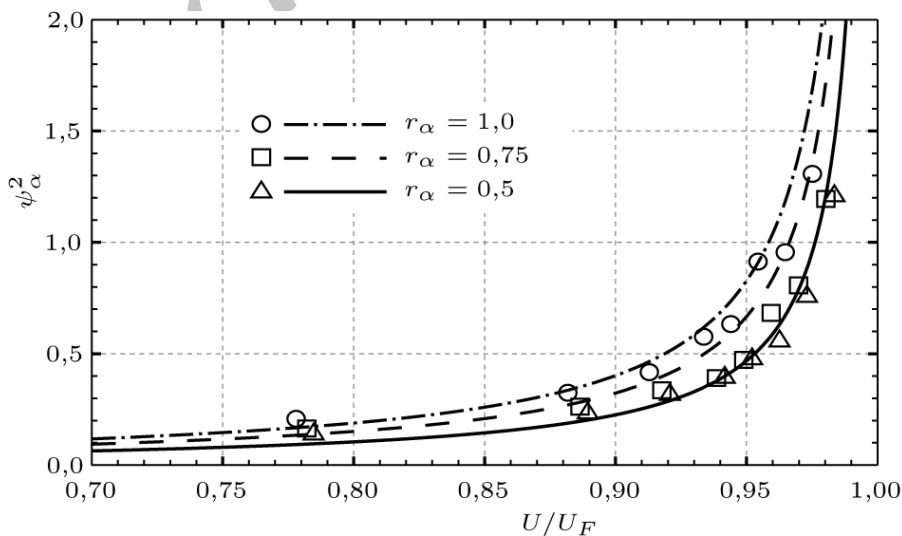
The ratios of the variances start from 1.0 when there is no wind, but as the positive aeroelastic damping dampens the structure, the effects of the self-feeding forces tend to

decrease the motions of the structure. Depending on the derivatives, different values of aeroelastic damping can act beside the structural damping, but their effect is always to soften the response of the structure to the turbulent wind forces. The structural damping has a huge impact on the results. The smaller the value the more sudden the flutter is, on an undamped structure the flutter appears with no antecedents. A high value of the structural damping decreases the effect of the aeroelastic damping (the ratio of them decreases), and the ratio of the variances tends toward the unity. The softness of the flutter [15] is the steepness of the total damping at the flutter, hard-type flutter has greater changes in the damping in function of the flutter speed. The softness is related to the absolute value (as this is negative) of the derivative of the total damping at the flutter velocity. The softness have an as great impact on the ratio of the variances as the damping itself. In the case of a hard-type flutter the total damping decreases rapidly, the ratio of the variances increases intensively.

An empirical formulation is fitted on the simulated data with the concept formulated previously as: it should be a function of the relative wind speed and should have infinite value at the flutter speed. The mass and radius of gyration ratios should be compared to the aerodynamic mass represented by the derivatives H_4^* and A_3^* at the flutter reduced velocity, and the derivative of the total damping should be in ratio of the damping. A formulation for the ratio of the angular motions is given in the form

$$\Psi^2 = \frac{1}{U_F^{C_1}} \frac{C_2}{\left(\frac{U}{U_F}\right)^{\frac{0.02\delta'}{\delta_s}} - 1} \left(\frac{A_3^*(U_{red})}{\mu \pi r_\alpha}\right)^{C_3} \tag{16}$$

where U is the average wind speed, U_F is the flutter speed determined on the undamped structure by spectral analysis, δ' is the derivative of the total damping at the flutter speed, $U_{red} = U_F / (\omega_F B)$ is the flutter reduced velocity and ω_F is the flutter frequency. C_1 , C_2 and C_3 are constants to be determined by fitting, which resulted all of them be 1.0.



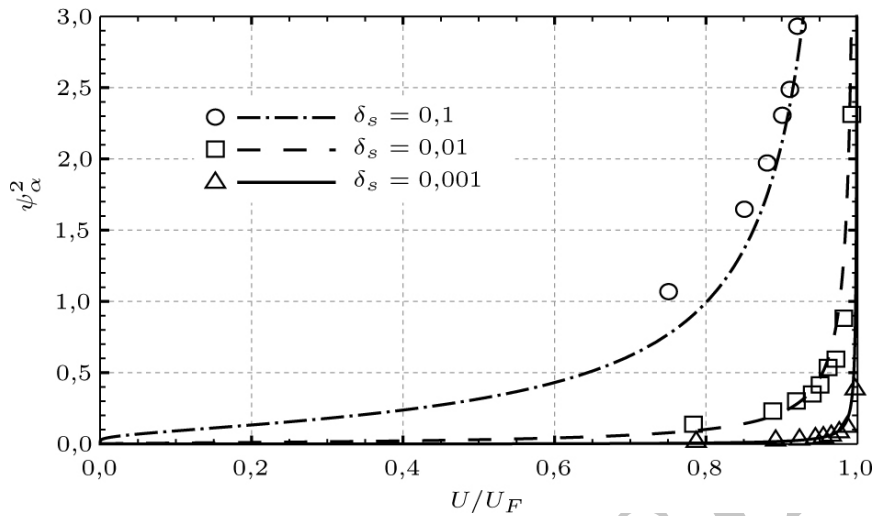


Figure 3. The fitted formula and the data of the squared ratio of the variance with/without self-feeding forces, with different settings of the parameters. Top: $\mu=10$, $\varepsilon=2.5$, $B=5$ m, $\omega_{0h}=1$ rad/s, $\delta_s=0.01$, below: $\mu=10$, $\varepsilon=2.0$, $B=5$ m, $r_a=0.5$, $\omega_{0h}=1$ rad/s

The fit of the formula is shown in Figure 3 with different structural parameters, an acceptable fit is concluded. The formula proposed is constrained to be used in the neighbouring of the flutter speed only. The fitting could be made more precise by taking into account the change in the flutter derivatives representing the mass (or stiffness) of the treated motion (A_3^* in the present case), estimating it by a linear approximation around the flutter speed. The flutter derivative accorded to the aeroelastic damping is taken into account in the derivative of the damping and the flutter speed, as is the case of the coupling effect too.

3.3 Flutter softness

Approximating the flutter derivatives by a polynomial form

$$H_i^*(U_{red}) = \sum_{j=1}^n h_{ij} U_{red}^j \quad A_i^*(U_{red}) = \sum_{j=1}^n a_{ij} U_{red}^j \quad (17)$$

results their derivatives according to wind speed U be

$$H_i^{*'} = \left(\frac{1}{U} + \frac{\varepsilon_F'}{\varepsilon_F} \right) \sum_{j=1}^n j h_{ij} U_{red}^j \quad A_i^{*'} = \left(\frac{1}{U} + \frac{\varepsilon_F'}{\varepsilon_F} \right) \sum_{j=1}^n j a_{ij} U_{red}^j \quad (18)$$

where h_{ij} and a_{ij} are constants, $\varepsilon_F = \omega_{0\alpha} / \omega_F$ is the flutter frequency ratio of the eigen torsional and the flutter frequencies, $()'$ is the derivation according to the wind velocity U . If an only second order approximation is used the derivative of the damping from the complex eigenvalue analysis can be expressed in function of the structural parameters and the flutter derivatives, and can be represented as in Figure 4.

The polynomial representation of the flutter derivatives does not allow simulating the

zeroes, nevertheless, qualitative conclusions can be made in regard to the softness of the flutter. The lower the derivative of the damping is, the softer the flutter is. The flutter is softer as the mass ratio increases and also as the dimensionless radius of gyration increases. These conclusions are asserted by analyses on the flutter derivatives of a thin airfoil and of the Hardanger Bridge [17]. The ratio ϵ of the eigenfrequencies acts similarly, the softness is proportional to it.

The softness can be used in practice as a help in the decision for an eventual bridge design: what kind of structural changes are needed to increase the flutter speed. In case of a soft type flutter (case of footbridges) the slight changes in the structural damping influence highly the flutter speed, while for hard type flutter other structural changes are also need to obtain the same increment.

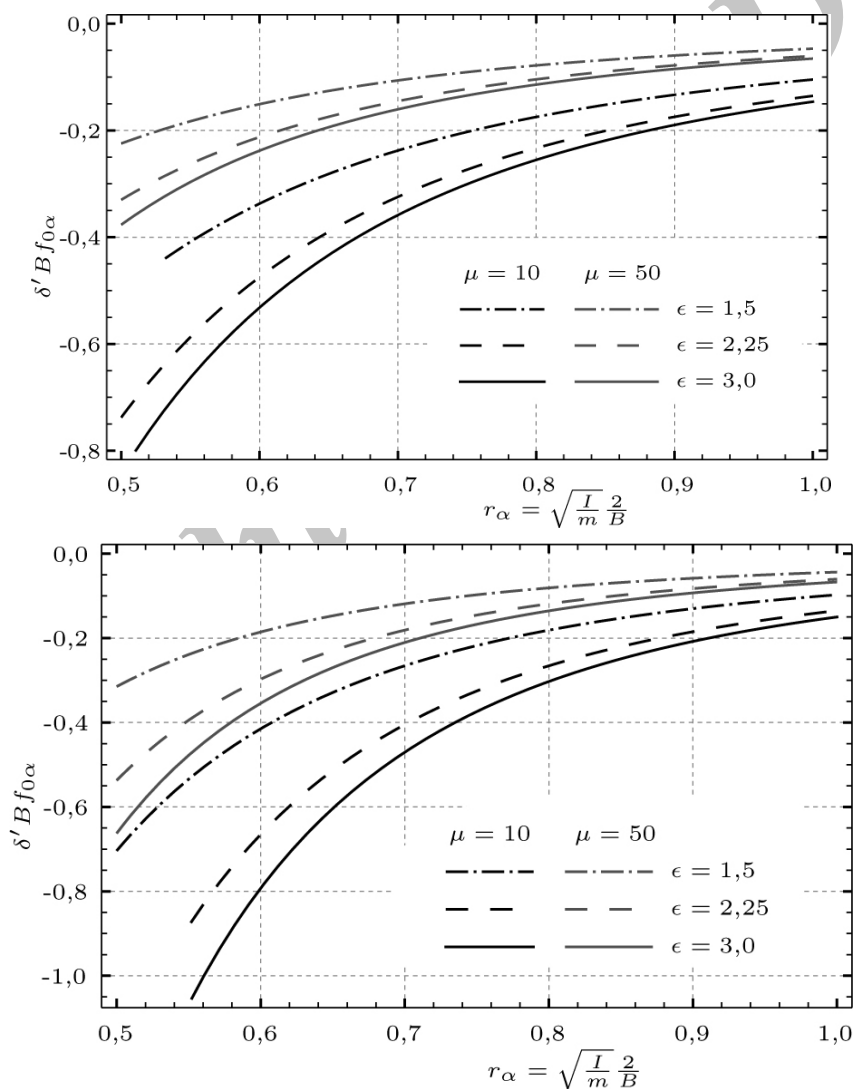


Figure 4. The derivative of the total damping (softness) at flutter velocity for a thin airfoil (top) and the Hardanger Bridge (below)

4. CONCLUSIONS

The paper has presented a framework to determine the influence of the self-feeding forces over the buffeting forces on a 2DOF section-model. The ratio of the displacement variances for the two situations, the buffeting forces with and without the self-feeding forces, has been investigated with the airfoil flutter derivatives.

The proposed general definition for the flutter speed is based on the changes of the variances in function of the length of the time interval considered. This definition is applicable to the results of the time domain analysis. The comparison of the flutter speed determined this manner with the complex eigenvalue analysis has shown good agreement.

The investigation has pointed out that well below the flutter speed the positive aeroelastic damping decreases significantly the structural responses. It is remarked that the squared ratio takes value less than 1.0, and thus the analogy with the stability of the axially compressed columns (Southwell method) has been declined. It is underlined that the variances of heave and torsional motions differ in accordance with the (mainly) heave or torsional type of the flutter. The same holds for the ratios.

The proposed formulation for the ratio of the variances has revealed the importance of the structural damping and the softness of the flutter, which is defined as the measure of how fast the total damping is changing in function of the wind speed at the flutter velocity, to the impact of the self-feeding forces over the buffeting ones.

The proposed method for determining the softness of the flutter has demonstrated how the structural parameters affect the softness of the flutter, and that the flutter derivatives control how the former act on it. Notably the ratio of the eigenfrequencies has opposite effects on the softness for the two flutter derivatives considered, while the mass ratio and the dimensionless ratio of gyration acts in a similar way for both cases.

Acknowledgements: This work is connected to the scientific program of the “Development of quality-oriented and harmonized R+D+I strategy and functional model at BME” project. This project is supported by the New Széchenyi Plan (Project ID: TÁMOP-4.2.1/B-09/1/KMR-2010-0002).

REFERENCES

1. Theodorsen T. General theory of aerodynamic instability and the mechanism of flutter, tech. rep. 496, *National Advisory Committee for Aeronautics*, 1935.
2. Klöppel K, Thiele F. Modellversuche im Windkanal zur Bemessung von Brücken gegen die Gefahr winderregter Schwingungen, *Der Stahlbau*, **36**(1967) 353–65.
3. Scanlan RH, Tomko JJ. Airfoil and Bridge Deck Flutter Derivatives, *Journal of the Engineering Mechanics Division*, **97**(1971) 1717–37.
4. Simiu E, Scanlan RH. Wind Effects on Structures: Fundamentals and Applications to Design, Wiley, 1996.
5. Petrini F, Giuliano F, Bontempi F. Comparison of time domain techniques for the evaluation of the response and the stability in long span suspension bridges, *Computers*

- & Structures*, **85**(2007) 1032–48.
6. Chen X, Matsumoto M, Kareem A. Aerodynamic coupling effects on flutter and buffeting of bridges, *Journal of Engineering Mechanics*, **126**(2000) 17–26.
 7. Chen X, Matsumoto M, Kareem A. Time domain flutter and buffeting response analysis of bridges, *Journal of Engineering Mechanics*, **126**(2000) 7–16.
 8. Kareem A. Numerical simulation of wind effects: A probabilistic perspective, *Journal of Wind Engineering and Industrial Aerodynamics*, **96**(2008) 1472–97.
 9. Carassale L, Solari G. Monte Carlo simulation of wind velocity fields on complex structures, *Journal of Wind Engineering and Industrial Aerodynamics*, **94**(2006) 323–39.
 10. Solari G, Tubino F. A turbulence model based on principal components, *Probabilistic Engineering Mechanics*, **17**(2002) 327–35.
 11. Li Y, Kareem A. ARMA representation of wind field, *Journal of Wind Engineering and Industrial Aerodynamics*, Part 1, **36**(1990) 415–27.
 12. Li Y, Kareem A. ARMA systems in wind engineering, *Probabilistic Engineering Mechanics*, **5**(1990) 49–59.
 13. Davenport AG. Buffeting of a suspension bridge by storm winds, *Journal of the Structural Division*, **88**(1962) 233–64.
 14. Solari G, Piccardo G. Probabilistic 3-D turbulence modeling for gust buffeting of structures, *Probabilistic Engineering Mechanics*, **16**(2001) 73–86.
 15. Salvatori L, Spinelli P. Effects of structural nonlinearity and along-span wind coherence on suspension bridge aerodynamics: Some numerical simulation results, *Journal of Wind Engineering and Industrial Aerodynamics*, **94**(2006) 415–30.
 16. Chen X, Kareem A. Revisiting multimode coupled bridge flutter: Some new insights, *Journal of Engineering Mechanics*, **132**(2006) 1115–23.
 17. Øiseth O, Sigbjörnsson R. An alternative analytical approach to prediction of flutter stability limits of cable supported bridges, *Journal of Sound and Vibration*, **330**(2011) 2784–2800.